

Ceria nanoformations in CO oxidation on Pt(1 1 1): Promotional effects and reversible redox behaviour

Y. Suchorski ^{*}, R. Wrobel ¹, S. Becker, B. Strzelczyk, W. Drachsel, H. Weiss

Chemisches Institut, Otto-von-Guericke-Universität Magdeburg, Universitätsplatz 2, D-39106 Magdeburg, Germany

Received 19 April 2007; accepted for publication 19 July 2007

Available online 25 August 2007

Abstract

A well-defined CeO_x/Pt(1 1 1) model catalytic system has been fabricated using the self-assembling of Ce adatoms on a Pt(1 1 1) surface with a subsequent oxidation of the nucleating Ce submonolayer (0.3 ML). The resulting system of the “inverse supported catalyst” type consists of CeO_x nanoformations (2D islands of 5–15 nm size and ~0.3 nm in height) more or less uniformly distributed over the Pt(1 1 1) surface. This CeO_x/Pt(1 1 1) system has been tested in the CO oxidation reaction where both the CO₂ production rate and the Ce oxidation state were monitored *in situ*. An enhanced reactivity and a remarkable shift of the bistable region of the reaction towards higher CO pressures were observed when compared to a clean Pt(1 1 1) surface. The CeO_x islands exhibit a pronounced redox behaviour that follows the hysteresis cycle of the reaction. The usefulness of such a type of the “inverse model catalyst” for studying the oxygen diffusion supply and the redox behaviour of ceria in the ceria-platinum catalysts is demonstrated.

© 2007 Elsevier B.V. All rights reserved.

Keywords: X-ray photoelectron spectroscopy; Scanning tunnelling microscopy; Surface chemical reaction; Metal–oxide interface; Oxidation; Carbon monoxide; Cerium oxide; Platinum

1. Introduction

Modern methods of surface nanofabrication such as electron-beam [1,2] or colloidal [3] lithography allow nowadays the creation of ordered arrays of small metal particles on a planar oxidic support. As in case of conventional supported metal cluster systems created by vapour deposition, such quasi two-dimensional systems can be well characterized morphologically by surface analytic techniques [4,5] and subjected to a detailed *in situ* kinetic investigation [6]. The nanofabrication provides the possibility to control not only the particle size but also the interparticle distances which are important e.g. for the interdiffusion of species between the particles. This facilitates the access to the fundamental catalytic problems such as size-effects [7], communication between the facets of single catalyst particles [8],

adsorbate-induced reshaping of catalyst particles [9], reactant supply via the support [10] or metal-support interaction [11]. As an alternative approach, “inverse supported catalysts” where oxide islands cover the metal catalyst surface may also significantly deepen our understanding of processes at the metal–oxide interface during an ongoing reaction [12].

Apart from the above-mentioned lithography and from the conventional deposition methods (see e.g. Refs. [10,11] for a review), the catalytically active nanoscaled structures can be fabricated purposely by creating conditions at which self-organization occurs, driven e.g. by a nonisotropic strain as in the case of the Cr/Pt(111) system [13]. Recently, ordered arrays of Ce atoms on the Ag(111) surface were created using the long-ranging adatom interaction mediated by the electronic system of the substrate [14].

The mentioned lateral adatom interaction results from long-ranging Friedel-type oscillating perturbations of the electron density by adsorbed atoms. It was first discussed

^{*} Corresponding author. Tel.: +49 391 67 18 824.

E-mail address: Yuri.Suchorski@OvGU.de (Y. Suchorski).

¹ On leave from Technical University of Szczecin, Poland.

by Koutecky already 50 years ago [15] and considered theoretically in the next two decades by Grimley and coworkers, Lau and Kohn as well Einstein and Schrieffer [16–19]. Almost contemporaneously, the implications of the substrate-mediated adatom interaction were observed experimentally by LEED for Li adatoms on W(112) [20] and by FIM for Re adatoms on W(110) [21], as well as for W–Pd and Re–Pd [22] and Re–Pd [23] atom pairs on W(110). A compilation of this early development including the dipole–dipole and elastically mediated non-oscillatory interactions is given in a comprehensive review [24].

Very recently long-ranging adsorbate interactions through the substrate electrons were evidenced for catalytically relevant adsorbates on noble-metal surfaces [25,26]. Kinetic Monte-Carlo simulations revealed a crucial role of such interactions in the nucleation of Ag islands on various fcc(111) surfaces [27,28] and in the self-assembling of initially randomly distributed Ce adatoms on Ag(111) [29]. Similar interaction mechanisms seem to be responsible for the formation of Ce nanostructures on Pt(111) or Rh(111) surfaces [30,31].

Assuming their successful subsequent oxidation, such self-assembled structures could be used for the creation of well-defined model systems for the above-mentioned “inverse supported catalysts”. Here ceria nanostructures are of particular interest, since the well-known ability of ceria to promote oxidation reactions via formation of oxygen vacancies as active interfacial centres is not entirely understood yet. Due to the presence of an extended metal–oxide interface such a well-defined ceria/Pt system might also serve helpful in studying the metal–support interaction.

As a test for this concept, it would be of interest to use such a system to mimic the CO oxidation on ceria-supported noble metal catalysts, a reaction which is important e.g. in the automotive exhaust treatment. Although ceria is known to influence the catalytic properties of Pt, promoting the low-temperature oxidation of CO and hydrocarbons [32], the atomistic details of this promoting function are still not well understood. The oxidation state of the used Pt/CeO_x catalysts seems to play an important role, as indicated by the observation that reduced (e.g. by H₂) samples are usually more active than pre-oxidized ones [33]. At the same time the (Ce³⁺ ↔ Ce⁴⁺) switch of the oxidation state in the Pt/CeO_x catalysts during the variation of the air-to-fuel ratio provides the oxygen storage function [34]. In practice, this helps to compensate transient deviations from the stoichiometric ratio. However, the yield of details of the (spill-over mediated) oxygen transport mechanism is still scarce despite of intensive experimental and modelling efforts [35]. The complex interplay between Pt, Ce, CO, and O species under reaction conditions is influenced by both electronic and structural contributions. Therefore, an adequate experimental study requires application of spectroscopic (e.g. XPS) and topographic (e.g. STM) techniques.

In the present paper we report the fabrication of a well-defined CeO_x/Pt(111) model system assembled using the indirect interaction of Ce adatoms on a Pt(111) surface. The promoting effect and the reversible redox behaviour of CeO_x nanoformations on Pt(111) is studied *in situ* during the ongoing CO oxidation reaction.

2. Experimental

All experiments were performed in an UHV surface analysis system operating at base pressures <10⁻¹⁰ mbar. The multipurpose apparatus provides among others the possibility for X-ray photoelectron spectroscopy (XPS; SPECS, Phoibos-150), scanning tunnelling microscopy (STM; Omicron NanoTechnology, VT-AFM/STM), combined Auger electron spectroscopy and low energy electron diffraction (AES, LEED; SPECS, ErLEED 150), and mass spectrometry (MS; MKS Instruments, VacCheck). During *in situ* monitoring of the CO oxidation, the differentially pumped UHV chambers were run as constant flow reactors by admitting the reactive gases (CO, O₂) via leak valves from constant pressure reservoirs.

The Pt(111) single crystal sample was a 1 mm thick disk of 10 mm in diameter. The standard surface cleaning procedure consisted in 1.5 keV argon ion sputtering at room temperature followed by annealing in oxygen (6 × 10⁻⁸ mbar) at 750 K and flashing in UHV to 1050 K. After several repetitions of the above procedure no contamination could be detected by XPS and a sharp hexagonal LEED pattern with low background was observed. The corresponding STM images show flat 20–50 nm wide terraces (see inset in Fig. 1). The cerium evaporation rate was adjusted to 0.25 ML/min as was estimated by independent experiments by AES analysis of Ce-submonolayers on a Cu(111) single crystal surface.

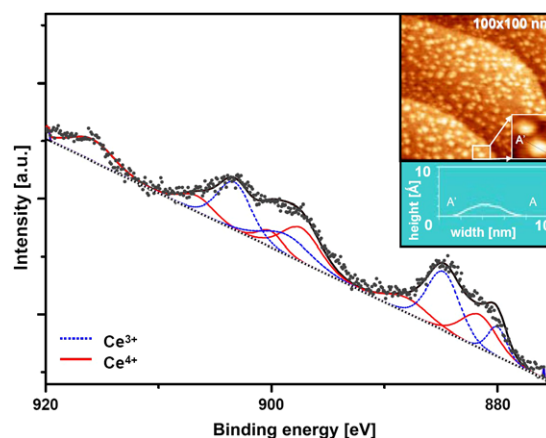


Fig. 1. Typical Ce 3d XP spectrum of the CeO_x/Pt(111) system as obtained by partial oxidation of a Ce submonolayer (0.3 ML, deposited at 125 K) in oxygen (20 L, $p_{O_2} = 1.3 \times 10^{-6}$ mbar, during warming-up from 125 to 300 K). The deconvolution of the spectra provides an average Ce oxidation state of 3.5 in the CeO_x islands. The inset shows a corresponding STM image and a typical CeO_x island profile. The shape of the Pt terraces remains unchanged during the CeO_x island fabrication.

The XPS spectra (pass energy 10 eV, step size 0.1–0.2 eV) were recorded with a 150 mm hemispherical energy analyzer using a Mg K α (1253.64 eV) X-ray source for the excitation. The CO oxidation on the clean Pt(111) single crystal surface and on the CeO $_x$ /Pt(111) system was monitored via the $m/z = 44$ (CO $_2$) mass spectrometer signal.

3. Results and discussion

Earlier attempts to promote the Pt(111) surface with Ce submonolayers have manifested the influence of Ce on the adsorption of carbon monoxide and oxygen but the details of the role of coadsorbed Ce in the reactivity of Pt surfaces are still not entirely understood [36,37]. The problems are caused mainly by interfacial Ce–Pt alloying at elevated temperatures which makes difficult the separation of the coadsorption- and substrate-effects [36–38].

To suppress the Ce–Pt alloy formation in present experiments, the Ce was deposited on a Pt sample cooled to 125 K. Immediately after deposition of 0.3 ML Ce oxygen was introduced at 10^{-6} mbar and the sample was simultaneously heated to 300 K. It is expected that oxygen adsorption may act as a kind of stabilizer for the nucleating Ce islands due to CeO $_x$ formation [38]. After exposure to ≥ 20 L of oxygen (usually, the oxygen uptake for Ce submonolayers on Pt saturates below 17 L [38]) the sample was investigated by XPS and, consequently, its surface topography was studied with STM. The corresponding STM images confirm the formation of dense CeO $_x$ islands of 5–15 nm size more or less uniformly distributed over the Pt(111) surface (Fig. 1). The high resolution XP spectra for the Ce 3d region shown in Fig. 1 provide the (spatially) averaged oxidation state of Ce in these nanoformations.

It has to be noted, that the determination of the Ce oxidation state in submonolayer CeO $_x$ formations is still difficult despite the great deal of work devoted to the electronic structure of ceria and similar compounds [39–41]. Apart from the low intensity of the XP signal, the difficulties result mainly from the particular features in the Ce 3d spectra which are related to multielectronic processes caused by the f-character of the O 2p valence electrons (initial state effect) and to a screening effect of the core-holes left by photoemitted electrons (final state effect) [42,43]. In the case when both oxidation states (Ce $^{3+}$ and Ce $^{4+}$) are present, the above effects lead to a complicated spectrum with overlapping peaks, where a total of 30 parameters, namely the peak positions, relative peak intensities and the FWHMs for each of 10 peaks in 3d spectra needs to be considered. In the present work the effective oxidation state of Ce was determined by correlation of the XPS data with those for reference samples CeO $_{2-x}$ with a known oxidation state. As reference samples Ar $^+$ -sputtered CeO $_2$ powder was used, where in UHV oxygen atoms in the surface region are preferentially released under the impact of Ar $^+$ ions. Details of the calibration procedure and the determination of the Ce oxidation state can be found elsewhere

[44]. From the Ce 3d XP spectra in Fig. 1 an average Ce oxidation state of 3.5 in the freshly prepared CeO $_x$ formations was obtained.

Immediately after its characterisation with XPS and STM the CeO $_x$ /Pt(111) system was subjected to an *in situ* kinetic investigation of the CO oxidation reaction. Fig. 2 shows the CO $_2$ production rate R_{CO_2} over the Pt(111) single crystal surface in comparison to the one above the CeO $_x$ /Pt(111) surface, both exposed to a constant partial pressure of oxygen (1.3×10^{-6} mbar) while the CO partial pressure is cyclic varied. The resulting $R_{CO_2}(p_{CO})$ curves exhibit a hysteresis for both the CO/O/Pt(111) and CO/O/CeO $_x$ /Pt(111) reaction systems. This is characteristic for a bistable reaction behaviour caused by the asymmetric inhibition of the dissociative oxygen adsorption by CO: Since O $_2$ needs two adsorption sites per molecule and can hardly adsorb on a densely CO-covered surface (CO, in turn, can easily adsorb on the oxygen-precovered surface), two stable states of the reaction system, with high and low reactivity, coexist over a range of operating conditions [45]. The bistable behaviour of the CO oxidation is well studied for Pt(111) [46] single crystal surfaces. Our studies on the nanofacets of Pt field emitter tips [47] as well as theoretical modelling [48] revealed that this inherent property of a monomer–dimer Langmuir–Hinshelwood reaction remains valid also for nano-sized reaction systems and is limited only by fluctuation-induced effects [49]. Recent experiments with cluster-oxide systems and with highly-dispersed Pt-on-ceria catalysts convincingly confirm these findings [50,51].

As Fig. 2 demonstrates, the presence of the CeO $_x$ islands shifts the bistability region remarkably towards higher CO pressures and increases the reactivity (CO $_2$ production rate) despite of the evident blocking effect (occupancy of active Pt sites by CeO $_x$ islands). The simplest explanation of the shift-effect would be the modified electron density at the

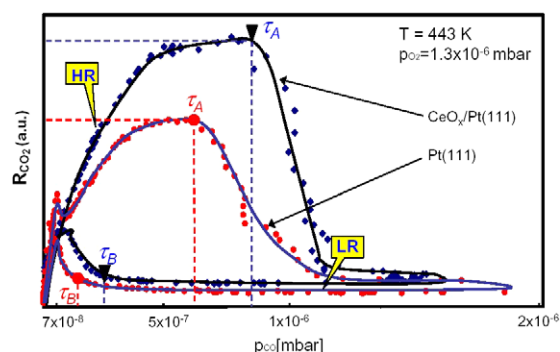


Fig. 2. Hysteresis in the CO $_2$ production rate R_{CO_2} as obtained upon cyclic variation of the CO partial pressure for constant oxygen pressure $p_{O_2} = 1.3 \times 10^{-6}$ mbar at $T = 443$ K. A bistable region is located between the monostable regions of high reactivity (HR) at low CO partial pressure and of low reactivity (LR) at high CO partial pressure, correspondingly. τ_A and τ_B mark the CO pressures at which the kinetic transitions occur. In comparison to the bare Pt(111), R_{CO_2} is significantly enhanced for the CeO $_x$ /Pt(111) system. The CO $_2$ production rate was evaluated from the relative changes in the CO $_2$ partial pressure (base pressure $< 10^{-10}$ mbar).

Pt surface along the perimeter of CeO_x islands (at the Pt– CeO_x interface). Our previous experiments with various Pt surfaces predosed with Li and Dy submonolayers have demonstrated that the coadsorption of electropositive adatoms shifts the bistability region in the CO oxidation on Pt towards higher CO pressures [47,52,53]. This is due to the coadsorbate-induced enhancement of the sticking coefficient of oxygen (see e.g. Ref. [54]) which can be interpreted as a purely electronic effect caused by the extension of the local electron density farther away from the surface [55]. As a result, the precursor potential as well as the dissociation barrier height for molecularly adsorbed species is modified [56,57]. This influences the adsorption/desorption equilibria of CO and molecular O_2 in favour of oxygen.

In the present case the modified electron density is restricted to adsorption sites along the borders of the CeO_x islands, a rather minor part of the total active area. This suggests that the additional oxygen supply may originate via diffusion from the CeO_x formations, similarly as suggested for a Pt/ CeO_x model catalyst prepared by electron-beam lithography [58]. An alternative mechanism comprising CO oxidation over the CeO_x islands can be rather neglected under the given conditions as was shown in Refs. [51,58] for samples containing CeO_x layers only. Certain contribution of the CO diffusion supply (via spill-over mechanism) from CeO_x islands to the Pt surface can not yet be excluded.

For both the number of modified adsorption sites and for the oxygen diffusion supply the role of the islands area and the islands perimeter line seems to be important and has to be studied. This can be easily done for the present system by varying the initial Ce coverage and will be addressed in forthcoming experiments. Such studies would also allow to evaluate the (physically meaningful) local increase of the catalytic activity, since a semi-quantitative estimation from the data of Fig. 2 (enhancement by factor of ~ 2 at $p_{\text{CO}} = 6.5 \times 10^{-7}$ mbar when normalized by the “uncovered” Pt(111) area) contains a rather rough average over the inhomogeneously active surface.

The enhanced activity observed for our CeO_x/Pt system in CO oxidation when compared to the clean Pt(111) surface is in accord with other observations [59] and can be attributed to the enhanced O_2 dissociation rate at the CeO_x/Pt interface. The interface step height of ~ 3 Å (see inset in Fig. 1) may provide an inhomogeneity which is sufficient to significantly facilitate the O_2 dissociation. Recently an enhanced CO oxidation rate was observed caused by a noticeable increase of the oxygen dissociation rate on steps of the Pt(411) surface [60]. The particular role of the island boundaries in CO adsorption, suggested recently for the ceria/Rh(111) system fabricated by reactive evaporation of Ce on Rh(111) [61], will be proven for our system soon in a detailed XPS study.

A possible electronic contribution to the increased reaction rate due to Ce–Pt alloy formation can be excluded: our experiments with intentionally created Ce–Pt alloy system (via annealing of the Ce submonolayer) have shown a re-

duced reaction rate in comparison to clean Pt(111) due to the blocking of active sites.

The oxidation state of Ce in the CeO_x islands was monitored *in situ* during the ongoing reaction and a pronounced redox behaviour was observed. Fig. 3 shows the corresponding XP spectra at various steady states of the reaction (high reactivity vs. low reactivity). As can be seen the Ce oxidation state is directly related to the hysteresis cycle of the reaction changing from 3.9 (high reactivity branch) to 3.6 (low reactivity) and *vice versa*. Similarly as in the ceria-supported catalysts, or in corresponding nano-fabricated model systems [59], oxygen seems to spill over from the Pt surface to the CeO_x islands increasing the Ce oxidation state ($x \rightarrow 2$) during the run through the high reactivity (oxygen reach) branch of the reaction and to spill back to the Pt surface during the low reactivity branch ($x \rightarrow 1.8$). Our experimental set-up provides the possibility to study the kinetic details of this process, which also will be done in future studies.

Finally, it should also be noted that the stability problem related to reshaping of the Pt particles in conventional

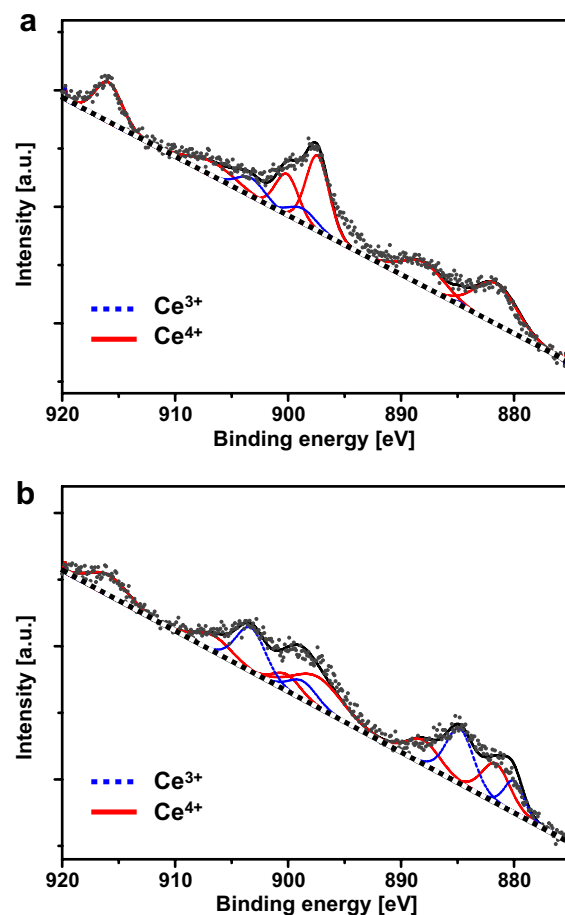


Fig. 3. XPS monitoring of the redox behaviour of the CeO_x islands during the hysteresis cycle of the CO oxidation. (a) Ce 3d XP spectrum for the $\text{CeO}_x/\text{Pt}(111)$ as measured at the point marked by arrow HR in the hysteresis cycle in Fig. 2. Spatially averaged Ce oxidation state: 3.9. (b) Same as in (a) but at the point marked by arrow LR. Corresponding Ce oxidation state: 3.6.

Pt/CeO_x model catalysts (see e.g. Ref. [59]) during the ongoing reaction does not appear in our case. The Pt(111) structure between the CeO_x islands survives the cyclic catalytic operation.

4. Summary

We have shown that a well-defined CeO_x/Pt(111) “inverse supported catalyst” model system can be assembled by exploiting the indirect interaction of Ce adatoms deposited at low temperature on the Pt(111) surface with a subsequent oxidation of the nucleating Ce submonolayer upon warming-up to room temperature at low oxygen pressure. The resulting system consisting of CeO_x islands on Pt(111) has been characterised by XPS and STM. The performance of this model catalytic system was studied *in situ* for the CO oxidation reaction where both the CO₂ production rate and the Ce oxidation state were monitored. A remarkable shift of the bistable region towards higher CO pressures and an enhanced reactivity of the CeO_x/Pt(111) when compared to a clean Pt(111) surface were observed. The CeO_x formations exhibit a pronounced redox behaviour that is directly related to the hysteresis cycle of the reaction. In contrast to the conventional Pt/CeO_x model systems where Pt nanoformations are deposited on a CeO_x surface and where reshaping of the Pt particles during operation might occur, the present CeO_x/Pt(111) model system is structurally stable. The complementarity of such an “inverse” system to the conventional Pt/CeO_x systems (where Pt nanoformations are deposited on the CeO_x surface) as well as the easily achievable variation of the island perimeter makes the present system to a promising object for studying the mechanisms of the oxygen diffusion supply and the role of the CeO_x-Pt interaction.

Acknowledgements

R.W. and B.S. acknowledge the support by EU Contract HPRN-CT-2002-00191.

References

- [1] G.A. Somorjai, Appl. Surf. Sci. 121/122 (1997) 1.
- [2] A. Avoyan, G. Rupprechter, A.S. Eppler, G.A. Somorjai, Top. Catal. 10 (2000) 107.
- [3] L. Österlund, S. Kielbassa, C. Werdinius, B. Kasemo, J. Catal. 215 (2003) 94.
- [4] D.W. Goodman, J. Catal. 216 (2003) 213.
- [5] H.-J. Freund, N. Ernst, T. Risse, H. Hamann, G. Rupprechter, Phys. Stat. Sol. 87 (a) (2001) 257.
- [6] M. Laurin, V. Johánek, A.W. Grant, B. Kasemo, J. Libuda, H.-J. Freund, J. Chem. Phys. 122 (2005) 084713–084721.
- [7] M. Morkel, G. Rupprechter, H.-J. Freund, Surf. Sci. 588 (2005) L209.
- [8] H. Persson, P. Thormählen, V.P. Zhdanov, B. Kasemo, Catal. Today 53 (1999) 273.
- [9] V.P. Zhdanov, B. Kasemo, Surf. Sci. Rep. 39 (2000) 25, and references therein.
- [10] H.-J. Freund, N. Ernst, M. Bäumer, G. Rupprechter, J. Libuda, H. Kühlenbeck, T. Risse, W. Drachsel, K. Al-Shamery, H. Hamann, in: A.F. Carley et al. (Eds.), Surface Chemistry and Catalysis, Kluwer Academic/Plenum Publishers, New York, 2002.
- [11] H.-J. Freund, Surf. Sci. 500 (2002) 271, and references therein.
- [12] K. Hayek, M. Fuchs, B. Klötzer, W. Reichl, G. Rupprechter, Top. Catal. 13 (2000) 55.
- [13] L.P. Zhang, J. van Ek, U. Diebold, Phys. Rev. B 59 (1999) 5837.
- [14] F. Silly, M. Pivetta, M. Ternes, F. Patthey, J.P. Pelz, W.-D. Schneider, Phys. Rev. Lett. 92 (2004) 016101.
- [15] J. Koutecky, Trans. Faraday Soc. 54 (1958) 1038.
- [16] T.B. Grimley, Proc. Phys. Soc. 90 (1967) 751.
- [17] T.B. Grimley, S.M. Walker, Surf. Sci. 14 (1969) 395.
- [18] K.H. Lau, W. Kohn, Surf. Sci. 75 (1978) 69.
- [19] T.L. Einstein, J.R. Schrieffer, Phys. Rev. B 7 (1973) 3629.
- [20] V.K. Medvedev, A.G. Naumovets, T.P. Smereka, Surf. Sci. 34 (1973) 368.
- [21] T.T. Tsong, Phys. Rev. Lett. 31 (1973) 1207.
- [22] H.-W. Fink, K. Faulian, E. Bauer, Phys. Rev. Lett. 44 (1980) 1008.
- [23] F. Watanabe, G. Ehrlich, J. Chem. Phys. 95 (1991) 6075.
- [24] O.M. Braun, V.K. Medvedev, Sov. Phys. Usp 32 (1989) 328.
- [25] N. Knorr, H. Brune, M. Epplé, A. Hirstein, M.A. Schneider, K. Kern, Phys. Rev. B 65 (2002) 115420.
- [26] V.S. Stepanyuk, A.N. Baranov, D.V. Tsvilín, W. Hergert, P. Bruno, N. Knorr, M.A. Schneider, K. Kern, Phys. Rev. B 68 (2003) 205410.
- [27] K.A. Fichthorn, M. Scheffler, Phys. Rev. Lett. 84 (2000) 5371.
- [28] K.A. Fichthorn, M.L. Merrick, M. Scheffler, Phys. Rev. B 68 (2003) 04104.
- [29] N.N. Negulyaev, V.S. Stepanyuk, L. Niebergall, W. Hergert, H. Fangohr, P. Bruno, Phys. Rev. B 74 (2006) 035421.
- [30] U. Berner, K.-D. Schierbaum, Phys. Rev. B 65 (2002) 235404.
- [31] E. Napetschnig, M. Schmid, P. Varga, Surf. Sci. 556 (2004) 1.
- [32] A. Törnroona, M. Skoglundh, P. Thormählen, E. Fridell, E. Jobson, Appl. Catal. B 14 (1997) 131.
- [33] A. Holmgren, F. Azarnoush, E. Fridell, Appl. Catal. B 22 (1999) 49.
- [34] A. Trovarelli, Catal. Rev. Sci. Eng. 38 (1996) 439.
- [35] V.P. Zhdanov, B. Kasemo, Appl. Surf. Sci. 135 (1998) 297.
- [36] J. Tang, J.M. Lawrence, J.C. Hemminger, Phys. Rev. B 48 (1993) 15342.
- [37] C.J. Baddeley, A.W. Stephenson, C. Hardacre, M. Tikhov, R.M. Lambert, Phys. Rev. B 56 (1997) 12589.
- [38] D. Fargues, A. Gally, J.J. Ehrhardt, Thin Solid Film 252 (1994) 105.
- [39] A. Pfau, K.D. Schierbaum, Surf. Sci. 321 (1994) 71.
- [40] D.R. Mullins, S.H. Overbury, D.R. Huntley, Surf. Sci. 409 (1998) 307.
- [41] J. Holgado, G. Munuera, J.P. Espinos, A.R. Gonzales-Elipe, Appl. Surf. Sci. 158 (2000) 164.
- [42] E. Willoud, B. Delley, W.D. Schneider, Y. Baer, Phys. Rev. Lett. 53 (1984) 202.
- [43] O. Gunnarson, K. Schönhammer, Phys. Rev. B 28 (1983) 4315.
- [44] Y. Suchorski, J. Gottfriedsen, R. Wrobel, B. Strzelczyk, H. Weiss, Solid State Phenom. 128 (2007) 115.
- [45] G. Ertl, Adv. Catal. 37 (1990) 231.
- [46] M. Berdau, G.G. Yelenin, A. Karpowicz, M. Ehsasi, K. Christmann, J. Block, J. Chem. Phys. 110 (1999) 11551.
- [47] Y. Suchorski, R. Imbihl, V.K. Medvedev, Surf. Sci. 401 (1998) 392.
- [48] Y. Suchorski, J. Beben, R. Imbihl, E.W. James, Da-Jiang Liu, J.W. Evans, Phys. Rev. B 63 (2001) 165417.
- [49] Y. Suchorski, J. Beben, E.W. James, J.W. Evans, R. Imbihl, Phys. Rev. Lett. 82 (1999) 1907.
- [50] V. Johánek, M. Laurin, A.W. Grant, B. Kasemo, C.R. Henry, J. Libuda, Science 304 (2004) 1639.
- [51] J. Zarraga-Colina, R.M. Nix, Surf. Sci. 600 (2006) 3058.
- [52] V.K. Medvedev, Y. Suchorski, Surf. Sci. Lett. 364 (1996) L540.
- [53] Y.B. Losovyj, I.V. Ketsman, P.P. Kostrobij, Y. Suchorski, Vacuum 63 (2001) 277.
- [54] M.P. Kiskinowa, in: B. Delmon, J.T. Yates (Eds.), Poisoning and Promoting in Catalysis Based on Surface Science Concepts and Experiments, Elsevier, Amsterdam, 1992, and references therein.
- [55] P.J. Feibelman, D.R. Hamann, Surf. Sci. 149 (1985) 48.

- [56] A.C. Luntz, J. Grimbolt, D.E. Fowler, *Phys. Rev. B* 39 (1989) 12903.
- [57] V.D. Osovskii, Y.G. Ptushinskii, V.G. Sukretnyi, B.A. Chuikov, V.K. Medvedev, Y. Suchorski, *Surf. Sci.* 377/379 (1997) 664.
- [58] S. Johansson, L. Österlund, B. Kasemo, *J. Catal.* 201 (2001) 275.
- [59] S. Johansson, E. Fridell, B. Kasemo, *J. Catal.* 200 (2001) 370.
- [60] H.D. Lewis, D.J. Burnett, A.M. Gabelnick, D.A. Fischer, J.L. Gland, *J. Phys. Chem. B* 109 (2005) 21847.
- [61] S. Eck, C. Castellarin-Cudia, S. Surnev, K.C. Prince, M.G. Ramsey, F.P. Netzer, *Surf. Sci.* 536 (2003) 166.